Inhomogeneous Structure of Collapsed Polymer Brushes under Deformation

E. B. Zhulina,* T. M. Birshtein, and V. A. Priamitsyn

Institute of Macromolecular Compounds, Russian Academy of Sciences, 199004 St. Petersburg, Russia

L. I. Klushin

Department of Physics, American University of Beirut, Beirut, Lebanon

Received March 17, 1995; Revised Manuscript Received August 24, 1995[⊗]

ABSTRACT: The theory of the equilibrium structure and properties of a planar brush under poor solvent conditions subjected to normal deformations (stretching or compression) is presented. Using a scaling type analysis, we demonstrate that at moderate grafting densities the brush loses its lateral homogeneity and the grafted chains form aggregates (pinned micelles) with globular cores and extended legs connecting the core with the grafting surface. These micelles are stable in a rather wide range of grafting densities provided that the chains are long and the solvent is poor enough so that $\tau N^{1/2} \gg 1$. Scaling relations as well as diagrams of states are obtained. It is shown that the normal deformation of the brush alters boundaries of the micelle stability regime and leads to the rearrangement of the equilibrium micelle structure. Stretching leads to an increase in both the width of the stability region and the number of chains in a micelle whereas compression causes a decrease in these values. Different scenarios of brush deformation are predicted. Hysteresis effects in the processes of interaction between brushes are discussed.

I. Introduction

The equilibrium behavior of polymer brushes and brushlike systems in poor solvents attracts more and more attention at present.[1-15] This problem is of interest with respect to numerous practical applications including stabilization of dispersions, wetting phenomena in thin films, formation of inhomogeneous adsorbed layers, etc. From a theoretical point of view a polymer brush in a poor solvent is an example of a system capable of undergoing lateral microsegregation. The reason for this is a peculiar manifestation of polymer–polymer attractive interactions under constraint, namely, anchoring of the chain ends at the grafting surface. Contrary to the situation in solution, grafting of the free ends onto the surface prevents the system from segregating into two macrophases enriched with either solvent or polymer. However, microsegregation is possible when the brush splits into spatially separated regions (domains) enriched with one of the components (polymer or solvent). Thus, microsegregation manifests itself in the modulation of the polymer density along the surface and the formation of the so-called "bundled" phase.

Two approaches have been used to study the lateral density inhomogeneity in the polymer brushes. One of them is the linear stability analysis based on the random phase approximation (RPA).[9-11] This method allows one to determine the boundary in the phase diagram where the laterally homogeneous density profile loses stability. It also gives the wavelength of the most unstable mode which has the meaning of the size of the incipient density modulation. The method is accurate in the vicinity of the transition, where the modulation of the density profile is small and the chain conformation is almost ideal. However, it cannot describe equilibrium structures in the strong segregation limit, i.e. far from the transition point. Moreover, it does not discriminate between the stable and the metastable states.

The other approach is based on comparing the free energy of a homogeneous brush with that of micelle-like clusters.[7,8] The model of a micelle-like aggregate was proposed independently by one of us[7] and by Williams.[8] This model is most appropriate in the strong segregation limit, where the clusters are well-defined. Whereas the manuscript[7] focused mainly on the case of planar brush in a poor solvent, utilizing the blob concepts, the other publication[8] dealt with a melt brush of various geometries. Though the work of Klushin[7] was not published, the results were distributed throughout the scientific community in the form of a preprint, and citations to this work are found in further publications on the subject (see, for example, the paper of Yeung et al.[10]). The model implies that each cluster consists of a core enriched by collapsed polymer and the "legs", connecting the core to the grafting surface. The author of ref 7 suggested one call such aggregates "pinned micelles", emphasizing the fact that the end points of the "legs" are fixed at the surface, whereas Williams used the term "octopus micelles".[8] Though both names reflect the peculiarities of the micelle's structure, in this publication we would like to follow the original notation of ref 7 and use the term "pinned micelles" throughout the paper. The scaling analysis[7] demonstrated that pinned micelles are stable in a wide range of grafting densities and solvent strengths. The scaling prediction for the boundary separating the homogeneous brush from the pinned micelles for the case of flexible chains agrees with the numerical RPA calculations.[10]

Theoretical investigations[7-12] were focused mainly on the free, nondeformed brushes. The analysis of deformed brush deformation under stretching or shear implies the existence of a certain amount of bridging chains to which stretching force can be applied. These chains exist in various systems (e.g. block copolymer mesophases and mesogels) and play an important role in the process of deformation. Normal deformations (stretching and compression) of collapsed brushes was considered earlier.[16,17] However, the analysis was restricted only to laterally homogeneous structures.

[⊗] Abstract published in *Advance ACS Abstracts,* November 1, 1995.

0024-9297/95/2228-8612$09.00/0

In this paper we extend the analysis of brush deformation by taking into account the possibility of lateral microsegregation via the formation of pinned micelles. Using simple scaling arguments, we consider the equilibrium structure of normally deformed brushes in a poor solvent, focusing on the role of bridging chains. In section II we describe the model and briefly summarize the scaling arguments,[7] justifying the introduction of pinned micelles. In sections III and IV we analyze the rearrangements of the pinned micelles caused by the brush deformation and eventually construct a scaling-type diagram of states for our system (section V). In section VI we summarize the main results of this paper and discuss possible experimental verifications of our predictions. The fluctuational behavior of the system is discussed in the Appendix.

II. Undeformed Brush

Consider a planar brush of polymer chains consisting of $N \gg 1$ symmetrical units of size a, grafted onto the surface at the grafting density $1/s$. Chains are assumed to be flexible, i.e. their Kuhn segment A is of the order of the length of the chain unit a, $A/a = 1$. In this paper, we will use a as a unit length. The brush is immersed in a poor solvent so that the second virial coefficient of unit interactions is $v = -\tau = (T - \Theta)/\Theta < 0$ and $\tau N^{1/2} > 1$.

The latter condition implies that an individual polymer chain immersed in such a solution will have the conformation of a collapsed globule, its characteristic size R_- and the average concentration of units $\varphi_- = N/R_-^3$ being described by the well-known formulas

$$R_- \cong (N/\tau)^{1/3} \tag{1a}$$

$$\varphi_- \cong \tau \tag{1b}$$

Here we assume that the third virial coefficient of chain unit interaction is equal to 1. One can envision such a globule as a densely packed system of N_b thermal blobs of the size

$$\xi_- \cong 1/\tau \tag{2}$$

the average concentration of units inside the blob being $\varphi_- = \tau$.[18,19] Within each blob the chain obeys Gaussian statistics; i.e. the number of units in each blob is equal to ξ_-^2. The free energy of both intra- and interblob interactions is on the order of kT per blob, so that the volume free energy of a globule is given by

$$F_-/kT \cong -N_b \cong -N/\xi_-^2 \cong -N\tau^2 \tag{3}$$

The increase in the free energy due to the surface of the globule can be estimated as kT per each surface blob

$$F_s/kT \cong R_-^2/\xi_-^2 \cong N^{2/3}\tau^{4/3} \tag{4}$$

provided that the thickness of the surface layer is on the order of ξ_-.

Loose grafting of such globules onto the surface does not change the scaling dependencies (1)–(4). Throughout this paper we assume that the interaction of a chain unit with the surface can be repulsive, or even slightly attractive, but never exceeds the critical value, above which the adsorption of the chain on the surface starts. Under these conditions the grafted chain is negligible and the chain retains the same globular conformation.

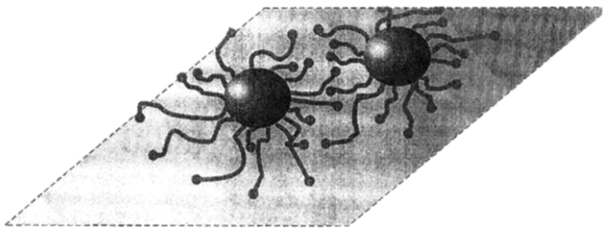

Figure 1. Schematic representation of pinned micelles.

As was demonstrated in ref 7, at dense grafting the brush retains lateral stability and its average concentration is given by (1b). At very sparse grafting the brush splits into separate globules described by (1). However, at moderate grafting densities separate globules aggregate and form the so-called pinned micelles (Figure 1). Formation of pinned micelles is favored by the gain in the surface free energy per chain in a micelle. However, such aggregation of globules is opposed by the geometrical constraint—anchoring of the chain ends at the surface. In order to overcome this constraint, each chain has to stretch. According to the scaling picture[20] of a stretched globule with a given end-to-end distance $D \gg R$, the chain produces a "leg", i.e. a string of n_L thermal blobs of length $L = n_L\xi_-$, whereas the rest of the chain forms a spherical core of radius $R \cong ((N - n_L\xi_-^2)/\tau)^{1/3}$, so that $D = L + R$. For moderate deformations $D \ll N\tau$, the size of the core $R \ll L$ and $D \approx L$, whereas $R \approx R_-$.

Let f be the number of chains in a micelle. Then the average length of the leg L scales as

$$L \cong D \cong \sqrt{sf} \tag{5}$$

where s is the grafting area per chain. Since each leg is a string of $n_L = D/\xi_-$ thermal blobs, it contains $n_L\xi_-^2 \cong D\xi_-$ chain units. Its total free energy contains the surface and the elastic contributions (both of the order of kT per blob) and therefore scales as

$$F_{leg}/kT \cong n_L \cong D/\xi_- \cong D\tau \cong s^{1/2}f^{1/2}\tau \tag{6}$$

The core comprising f chains has the radius

$$R \cong (fN/\tau)^{1/3} \tag{7}$$

and the corresponding surface free energy F_s is given by

$$F_s/kT \cong R^2/\xi_-^2 \cong f^{2/3}N^{2/3}\tau^{4/3} \tag{8}$$

The total free energy per chain in the micelle $F_m = F_{leg} + F_s/f$ scales as

$$F_m/kT \cong f^{1/2}s^{1/2}\tau + f^{-1/3}N^{2/3}\tau^{4/3} \tag{9}$$

Note that we excluded the free energy of volume interactions (eq 3) from consideration by taking it as a reference state and, as before, all numerical coefficients are omitted. The equilibrium value of f is obtained from the condition $\partial F_m/\partial f = 0$ to give

$$f \cong \tau^{2/5}N^{4/5}s^{-3/5} \tag{10}$$

Correspondingly, the radius R of the core, the total

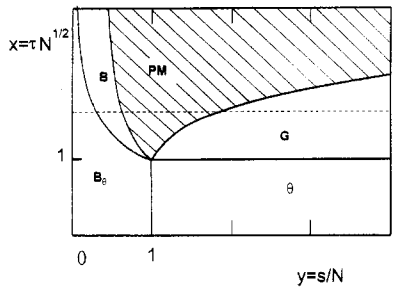

Figure 2. Scaling type diagram of state of a nondeformed brush: Regimes: G, individual globules; Θ, individual Gaussian chains; B_Θ and B, homogeneous brushes in Θ and poor solvent regimes, correspondingly; PM, pinned micelles.

dimension D of the micelle, and the free energy per chain scale as

$$\left.\begin{aligned} R &\cong N^{3/5}\tau^{-1/5}s^{-1/5} \\ D &\cong N^{2/5}\tau^{1/5}s^{1/5} \end{aligned}\right\} \quad (11)$$

$$F_m/kT \cong N^{2/5}\tau^{6/5}s^{1/5} \quad (12)$$

Comparing the free energies per chain in a micelle and in other possible structures (separate globules, homogeneous brush), we find the interval of grafting areas per chain $s_1 > s > s_2$, where micelles are stable.

The boundary

$$s_1 \cong N^{4/3}\tau^2 \cong R_-^{\,2}(N^{1/2}\tau)^{4/3} \quad (13)$$

separates the micellar regime and the regime of one-chain globules (mushrooms regime), whose free energy is given by (4). The boundary

$$s_2 \cong N^{1/2}\tau^{-1} \cong R_-^{\,2}(N^{1/2}\tau)^{-1/3} \quad (14)$$

separates the micellar regime from that of a homogeneous brush of thickness

$$H_- \cong N/s\tau \quad (15)$$

with the free energy per chain

$$F_-/kT \cong s/\xi^2 \cong s\tau^2 \quad (16)$$

Figure 2 presents the scaling type diagram in $x = \tau N^{1/2}$, $y = s/N$ variables. It summarizes the above results and includes also the additional Θ regions existing at small $\tau N^{1/2}$. Regions G and Θ correspond to individual chains (mushrooms) either globulized or forming ideal coils, respectively. Regions B_Θ and B correspond to a homogeneous brush in a Θ or a poor solvent, respectively, whereas the PM region corresponds to the regime of pinned micelles. An increase in s at fixed values of N and τ corresponds to the intersection of the diagram of Figure 2 along the dashed line. The parameters of the brush in various regions of the diagram are summarized in Table 1. Note that in the laterally inhomogeneous regimes G and PM the brush thickness is taken equal to the dimension of separate a globule R_- or a micelle R, respectively.

As follows from (13) and (14) and Figure 2, the micellar regime covers a broad interval of grafting areas provided $\tau N^{1/2} \gg 1$. The values s_1 and s_2 are, correspondingly, well above and well below the overlapping areas both for separated globules $s = R_-^{\,2}$ and for the Gaussian chains $s = N$. On approaching the s_1 boundary the number of chains per micelle decreases down to $f \cong 1$, whereupon the pinned micelles decompose into separate globules. At the s_2 boundary the size R of the micellar core becomes equal to the size D of the micelle as a whole, and the micelles coalesce into a homogeneous brush. Note that at $s \ll s_2$ the chains in this brush are stretched with respect to the Gaussian value $H > N^{1/2}$, but they have Gaussian dimensions $H = N^{1/2}$ at the boundary s_2. Thus, the condition $H > N^{1/2}$ is the scaling condition of brush lateral stability.

It is necessary to remember, however, that all the boundaries in Figure 2 are introduced as the lines of crossover between the different scaling regimes. In the present paper, we will not discuss the nature of the transitions between these regimes (in particular, whether they could be identified as phase transitions).

Table 1. Scaling Laws for the Parameters of the Brush in the Different Regimes of the Diagram in Figure 2 (F = Total Free Energy per Chain)

regions	H	R	D	F/kT
B	$N/s\tau$			$-N\tau^2 + s\tau^2$
G		$(N/\tau)^{1/3}$		$N^{2/3}\tau^{4/3} - N\tau^2$
PM		$N^{3/5}/\tau^{1/5}s^{1/5}$	$N^{2/5}\tau^{1/5}s^{1/5}$	$N^{2/5}\tau^{6/5}s^{1/5} - N\tau^2$
Θ		$N^{1/2}$		
B_Θ	$Ns^{-1/2}$			Ns^{-1}

III. Compressed Brush

Compression of a brush can be attained by pressing the surface covered by grafted polymer with a bare one. We consider first the compression of laterally inhomogeneous brushes.

Compression of an individual globule (region G in Figure 2) was considered earlier.[20] Here we summarize briefly the results which are relevant for the subsequent analysis. Let H be the (variable) distance between the surfaces. According to ref 20, normal compression of a globule leads to the variation in its shape from a sphere of radius R_- to a pancake of the thickness H and the radius

$$R \cong (N/H\tau)^{1/2} \quad (17)$$

This implies conservation of the average globular concentration φ_- and the blob size ξ_- (eqs 1 and 2).

At relatively weak compression the increase in the free energy is related mainly to the increase in the surface free energy

$$F_s/kT \cong (R^2 + RH)/\xi_-^{\,2} \cong N\tau/H + N^{1/2}H^{1/2}\tau^{3/2} \quad (18)$$

Only at very strong compression, $H \cong \xi_-$, does the entropy loss caused by the chain deformation start to dominate, and at even smaller H, the chain obeys the statistics of a strongly compressed chain in a Θ solvent. However, we will not consider here this range of deformations and restrict ourselves to the case $H \gg \xi_- \cong \tau^{-1}$.

Consider a pinned micelle of f chains with a pancake core of the thickness H and the radius

$$R \cong (Nf/H\tau)^{1/2} \quad (19)$$

As before, the equilibrium value of f can be obtained by balancing the surface free energy of the core and the free energy of stretched legs—strings of thermal blobs. The total free energy per chain in such a micelle, F_m, is obtained from eqs 18, 19, and 8 to give

$$F_m/kT \cong N\tau/H + f^{-1/2}N^{1/2}H^{1/2}\tau^{3/2} + f^{1/2}\tau s^{1/2} \quad (20)$$

Minimizing F_m with respect to f, one obtains

$$f \cong (\tau NH/s)^{1/2} \tag{21}$$

and, correspondingly,

$$R \cong N^{3/4}/(\tau sH)^{1/4} \tag{22}$$

$$D \cong (NHs\tau)^{1/4} \tag{23}$$

$$F_m/kT = \frac{N\tau}{H} + (NHs\tau^5)^{1/4} \tag{24}$$

Thus, compression of pinned micelles leads to the reorganization of their structure and to the corresponding change in thermodynamics: the number of chains f and the total size D of the micelle become smaller, whereas the lateral dimension of the pancake core R and the chain free energy F_m increase with decreasing H. As a result, compression leads eventually to the disappearance of the micellar structure. This may happen in two ways: At relatively sparse grafting, $s/N > 1$, decreasing H leads to a rapid decrease in f to $f \cong 1$ and, finally, the micelle splits into separate compressed globules. The boundary between the compressed pinned micelles and separate compressed globules can be obtained by equating the free energies F_s (eq 18) and F_m (eq 24) or by equating $f = 1$ in eq 21 to give

$$H_1 \cong sN^{-1}\tau^{-1} \tag{25}$$

With further compression, each chain retains the conformation of an individual compressed globule.

At relatively dense grafting, $s/N < 1$, F_m becomes equal to the surface free energy of a homogeneous brush and simultaneously D becomes of the order of R at a certain finite value of $f > 1$. This occurs at

$$H_2 \cong Ns^{-1}\tau^{-1} \tag{26}$$

Thus, at $H = H_2$, the brush loses its lateral inhomogeneity and transforms into a laterally homogeneous undeformed layer, provided $H_2 = H_-$ (eq 15). At $H < H_2$ we have a homogeneous compressed layer.

Compression of homogeneous brushes in poor and Θ solvents (regimes B and B_Θ in Figure 2) was already considered earlier.[17] In both cases the brush retains homogeneity and its local structure is determined by the correlation length $\xi \cong 1/\varphi$, where $\varphi = N/sH$ is the average volume fraction of polymer units in the gap between two surfaces. In both cases the brush is a densely packed system of Gaussian blobs of size ξ.

Thus, depending on the grafting density, compression of pinned micelles leads either to recovery of the lateral homogeneity of the brush ($s < N$) or to its splitting into individual compressed globules ($s > N$). The range of stability of pinned micelles decreases with compression and for a fixed value of H is given by

$$s_2\frac{N^{1/2}}{H} \cong \frac{N}{H\tau} < s < HN\tau \cong s_1\frac{H\tau^{1/3}}{N^{1/3}} \tag{27}$$

where s_1 and s_2 are given by eqs 13 and 14. The diagram of states of a compressed brush will be presented below (Figure 4) as a part of the general diagram for a deformed brush.

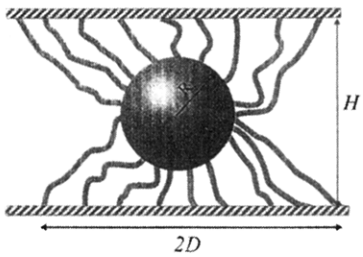

Figure 3. Schematic representation of stretched pinned micelles formed by bridging chains.

IV. Stretched Brush

Let us now pass to the case of a stretched brush. Stretching implies anchoring some free chain ends irreversibly on the second surface, i.e. the existence of bridging chains connecting both surfaces. Thus, in order to analyze the effect of stretching we modify our model by introducing the second planar surface which is attached to the covered surface by a constant fraction q of bridging chains, Figure 3. The distance H between the two surfaces is considered as a variable parameter. Such a model allows us to consider both stretching and compression of the brush and is more relevant to realistic systems, such as, for example, block copolymer mesophases and mesogels. In order to obtain the main features of the brush behavior we assume $q = 1$; i.e. we consider the situation when all chains form bridges. The effect of finite $q < 1$ on the brush structure will be investigated elsewhere.

Stretching of individual globules and laterally homogeneous layers in poor and Θ solvents was considered earlier in refs 17 and 20. Under stretching, both individual globules and densely grafted homogeneous brushes undergo a "phase" transition, forming a core filled with densely packed thermal blobs and the legs—strings of thermal blobs (see refs 17 and 20 for details). In the case of individual globules the core is spherical. For densely grafted brushes it was assumed that the core retains lateral homogeneity and has the shape of a planar layer parallel to the surfaces.

Let us investigate now the stretching of the brush in the pinned micelle regime. One can envision such a micelle as consisting of a spherical core in the middle of the gap, attached by equal numbers of legs to both surfaces, Figure 3. Since the length of the legs is affected by the distance H between the surfaces, the equilibrium parameters of the stretched pinned micelle will be sensitive to the distance H. For a micelle of f chains the average length of the leg is given by

$$L \cong \sqrt{sf + H^2} - R \tag{28}$$

where, as before, all numerical coefficients are omitted. Correspondingly, the free energy per leg scales as $F_{leg}/kT \cong L/\xi_-$. The surface free energy of the core is determined by (8) and the total free energy of a chain in the micelle is given by

$$F_m/kT \cong \tau\sqrt{sf + H^2} - \tau R + f^{-1/3}N^{2/3}\tau^{4/3} \tag{29}$$

Minimizing F_m with respect to f, one obtains

$$\frac{s}{\sqrt{sf + H^2}} \cong \frac{\tau^{1/3}N^{2/3}}{f^{4/3}}\left(1 + \frac{f^{2/3}}{N^{1/3}\tau^{2/3}}\right) \tag{30}$$

The power law dependences are obtained from (30) in the limiting cases $H^2 \ll sf$ and $H^2 \gg sf$. If $H^2 \ll sf$, we return to the scaling results (10)–(12) for the nondeformed micelles. For $H^2 \gg sf$ when the length of a leg is determined mainly by the distance H between the surfaces, one can neglect the sf term in (30). Depending on the ratio of the two terms in brackets on the right side of (30), we obtain two different scaling laws for $f \ll N^{1/2}\tau$ and $f \gg N^{1/2}\tau$.

If $f \ll N^{1/2}\tau$ (stretched pinned micelles 1, SPM1), neglecting the second term in brackets in (30), we obtain the number f of chains in a micelle

$$f \cong \tau^{1/4}N^{1/2}H^{3/4}s^{-3/4} \tag{31}$$

Correspondingly, the core size, the total lateral size of the micelle D, and the free energy per chain scale as

$$\left.\begin{aligned} R &\cong N^{1/2}H^{1/4}s^{-1/4}\tau^{-1/4} \\ D &\cong \sqrt{sf} \cong \tau^{1/8}s^{1/8}N^{1/4}H^{3/8} \\ F_m/kT &\cong \tau H + N^{1/2}H^{-1/4}\tau^{5/4}s^{1/4} \end{aligned}\right\} \tag{32}$$

The above scaling formulas result from a balance between the surface free energy of the core and the free energy of the legs. Note that just this case is realized for the undeformed system (section II), which allowed us to ignore R on the right side of (5).

If $f \gg N^{1/2}\tau$ (stretched pinned micelles 2, SPM2), neglecting the first term in brackets in (30), we obtain

$$\left.\begin{aligned} f &\cong N^{1/2}\tau^{-1/2}H^{3/2}s^{-3/2} \\ R &\cong N^{1/2}\tau^{-1/2}H^{1/2}s^{-1/2} \\ D &\cong N^{1/4}\tau^{-1/4}H^{3/4}s^{-1/4} \\ F_{in} &\cong \tau H - N^{1/2}\tau^{1/2}H^{1/2}s^{-1/2} \end{aligned}\right\} \tag{33}$$

In this case, the surface free energy of the core is unimportant, and the result follows from a delicate balance in the free energy of the legs which depends on both D and R. In both regimes the number of chains per micelle increases with H.

The boundary between SPM1 and SPM2 regions corresponds to

$$H \cong s\tau \tag{34}$$

The range of deformations where (31)–(33) are valid, is determined by the condition $H \gg D$, thus providing the boundary of the stretched pinned micelle regimes. For SPM1 and SPM2 we obtain correspondingly

$$H > N^{2/5}\tau^{1/5}s^{1/5} \tag{35}$$

$$H > N\tau^{-1}s^{-1} \tag{36}$$

Note that the thickness of the undeformed laterally homogeneous brush is just $H = N/s\tau$, (15). Hence it follows from (36) that the brush will lose the lateral homogeneity immediately upon stretching. We will discuss this question in more detail in the next section.

V. Diagram of States of the Deformed Brush

Figure 4 presents the scaling type diagram of the deformed brush in the $z = H/N\tau$ and $y = s/N$ coordinates. The equilibrium parameters of the brush and the relations for the boundaries are summarized in Tables 2 and 3. The dashed line in Figure 4 corresponds to the dimensions of a nondeformed system, (1), (11), and (15).

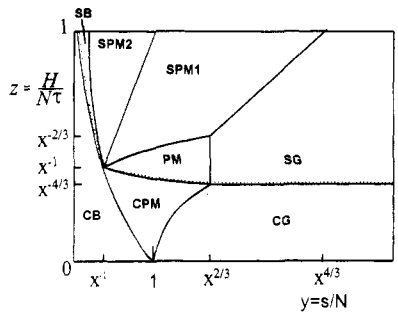

Figure 4. Scaling type diagram of state of a deformed brush, $x = N^{1/2}\tau \gg 1$. Dashed lines correspond to the dimensions of nondeformed systems. Regions: CB, CPM, and CG (compressed systems) homogeneous brush, pinned micelles, and globules, correspondingly; SB, SPM, and SG (stretched systems), laterally homogeneous brush, pinned micelles, and globules, correspondingly; PM, nondeformed pinned micelles.

Below the dashed line lie the regions of compressed individual globules (CG), compressed homogeneous brush (CB), and compressed pinned micelles (CPM). Above the dashed line the diagram shows several regions corresponding to stretched laterally inhomogeneous systems: SG, stretched individual globules; SPM1 and SPM2, stretched pinned micelles; PM, "nondeformed" pinned micelles.

All the regimes SG, SPM1, and SPM2 are limited from above by the boundary $H \cong N\tau$. This boundary corresponds to the totally stretched string of thermal blobs of an individual chain. Above this boundary the thermal blobs are deformed and the local chain structure is determined by the so-called stretching blob of the size $\xi_s \cong N/H < \xi_-$.[19] We do not discuss this regime here (see ref 20 for details). In the vicinity of this boundary in the SPM1 and SPM2 regions the number of chain units in the legs becomes comparable to that in the core. This leads to corrections in (31)–(33) for the number of chains in a micelle, where now N should be substituted by $(N - H/\tau)$. Correspondingly, in the vicinity of the upper boundary the number of chains per micelle

$$\begin{aligned} f &\cong \tau^{1/4}H^{3/4}s^{-3/4}(N - H/\tau)^{1/2} \quad \text{SPM1} \\ f &\cong \tau^{1/2}H^{3/2}s^{-3/2}(N - H/\tau)^{1/2} \quad \text{SPM2} \end{aligned} \tag{37}$$

diminishes with increasing H and becomes of the order of unity ($f \cong 1$) at $N - H/\tau \cong s^{3/2}\tau^{-1/2}H^{-3/2} \cong s^{3/2}\tau^{-2}N^{-3/2}$ (SPM1) and $N - H/\tau \cong s^3\tau^{-1}H^{-3} \cong s^3\tau^{-4}N^{-3}$ (SPM2). Thus the dependence $f(H)$ is nonmonotonic in the SPM regimes: it passes through a maximum in the vicinity of the boundary $H \cong N\tau$ and then decreases rapidly to zero.

The scaling approximation gives only micellar and globular regimes for the stretched brush. According to (36), the left boundary of the SPM2 region runs along the dashed line indicating the state of an undeformed, laterally homogeneous brush on the diagram in Figure 4. At this point, we will go beyond the scope of the scaling approximation and introduce an additional "stretched brush" regime (SB). We define the stretched brush as a system in which the regions of the polymer-rich phase of density φ_- form a continuous phase, as opposed to the picture of well-separated micelles in the SPM regime. The stretched brush does not have to be completely homogeneous: it is just that the volume fraction of the solvent-rich phase is too small to cause the splitting of the layer into separate micelles. Obvi-

Table 2. Scaling Laws for the Parameters of the Laterally Inhomogeneous Brush in the Different Regimes of the Diagram in Figure 4

regions	R	D	f	$(F/kT) + N\tau^2$
CPM	$N^{3/4}/(\tau s H)^{1/4}$	$(NHS\tau)^{1/4}$	$(\tau NH/s)^{1/2}$	$(N\tau/H) + (NHs\tau^5)^{1/4}$
PM	$N^{3/5}/\tau^{1/5}s^{1/5}$	$N^{2/5}\tau^{1/5}s^{1/5}$	$\tau^{2/5}N^{4/5}/s^{3/5}$	$N^{2/5}\tau^{6/5}s^{1/5} + (H^2\tau^{4/5}/N^{2/5}s^{1/5})$
SPM1	$N^{1/2}H^{1/4}/s^{1/4}\tau^{1/4}$	$\tau^{1/8}s^{1/8}N^{1/4}H^{3/8}$	$\tau^{1/4}N^{1/2}H^{3/4}/s^{3/4}$	$\tau H + N^{1/2}H^{-1/4}\tau^{5/4}s^{1/4}$
SPM2	$N^{1/2}H^{1/2}/s^{1/2}\tau^{1/2}$	$\tau^{-1/4}s^{-1/4}N^{1/4}H^{3/4}$	$\tau^{-1/2}N^{1/2}H^{3/2}/s^{3/2}$	$\tau H - N^{1/2}H^{+1/2}\tau^{1/2}s^{-1/2}$
CG		$(N/H\tau)^{1/2}$		$N\tau/H + N^{1/2}H^{1/2}\tau^{3/2}$
SG		$(N/\tau)^{1/3}$		$N^{2/3}\tau^{4/3} + \tau H$

Table 3. Crossover Boundaries between Different Regimes in the Diagram of Figure 4

boundary	equ
CB/SB, CB/CPM	$H \cong Ns^{-1}\tau^{-1}$
CPM/PM	$H \cong N^{3/5}\tau^{-1/5}s^{-1/5}$
PM/SPM	$H \cong N^{2/5}\tau^{1/5}s^{1/5}$
CPM/SG	$H \cong sN^{-1}\tau^{-1}$
PM/SG	$s \cong N^{4/3}\tau^{2/3}$
SPM/SG	$H \cong N^{-2/3}\tau^{-1/3}s$
CG/SG	$H \cong (N/\tau)^{1/3}$
SPM1/SPM2	$H \cong \tau s$

ously, the transition from the SB to the SPM regime is related to the percolation transition and is governed by the ratio of volume fractions for two microphases. A simple estimate shows that the brush has to be stretched by about a factor of 2 in order to develop isolated micelles. This defines a relatively narrow window for the SB region between the dashed line and the SPM2 boundary of the diagram in Figure 4. Both boundaries of the SB regime scale in the same way but differ in coefficients. Our scaling approach cannot detect this region due to systematical neglection of the numerical coefficients.

Note that along the SPM2/SB boundary as well as the boundary CPM/CB one has $R = D$. At the SPM2/SB boundary, $R \cong D \cong N/\tau s$, whereas at the CPM/CB boundary $R \cong D \cong N^{1/2}$. The left boundary of the PM region collapses to the single point $s \cong N^{1/2}\tau^{-1}$, $H \cong N^{1/2}$ comprising the contact points of the six regions.

The right boundaries of the regions SPM1 and PM are determined by the condition $f \cong 1$ to give

$$H \cong N^{-2/3}\tau^{-1/3}s \tag{38}$$

$$s \cong N^{4/3}\tau^{2/3} \tag{39}$$

correspondingly.

The diagram of Figure 4 shows that stretching of the brush increases the range of stability of micellar structures. At fixed H ($N\tau > H > N^{2/3}\tau^{1/3}$) the interval of stability for the stretched pinned micelles is given by

$$s_2N^{1/2}H^{-1} \cong NH^{-1}\tau^{-1} < s < N^{2/3}H\tau^{1/3} \cong s_1HN^{-2/3}\tau^{-1/3} \tag{40}$$

where s_1 and s_2 are given by (13) and (14). On the contrary, the compression diminishes the interval of stability of micelles (see eq 27).

VI. Discussion

1. Pinned Micelles in a Brush under Deformation. The above results describe the equilibrium structure and properties of a planar brush under poor solvent conditions subjected to normal deformations (stretching or compression). Using the scaling type analysis, we demonstrated that at moderate grafting densities the brush loses its lateral homogeneity and the grafted chains form aggregates—the so-called pinned micelles. These micelles are stable in a rather wide range of grafting densities provided that the chains are long and the solvent is bad enough so that $x = \tau N^{1/2} \gg 1$. Estimates showing that under these conditions the aggregates are well-defined and it is possible to use simple scaling arguments to describe their internal structure are given in the Appendix.

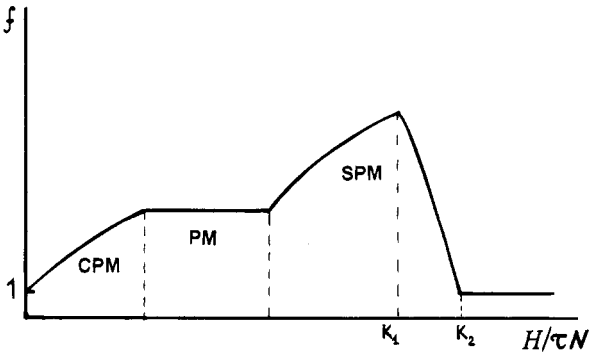

Figure 5. Schematic dependence of the number of chains in a micelle via deformation, $k_2 > k_1$, k_1, $k_2 \sim 1$.

Our analysis is based on the idea[7] that pinned micelles are spatially inhomogeneous: their core of the size R retains the concentration of a polymer globule, whereas the corona of the lateral size D is enriched by the pure solvent. Legs connecting the core with the grafting surface occupy only a small fraction of the crown space. Thus, one has two length scales, R and D, characterizing the modulation of the polymer concentration along the surface. For nondeformed pinned micelles $D \cong \tau^{1/5}s^{1/5}N^{2/5}$ and $R \cong \tau^{-1/5}s^{-1/5}N^{3/5}$, so that within the stability range $D \gg R$. For example at $s/N = 1$ (in the middle of the stability range) $R/D \approx (\tau N^{1/2})^{-2/5}$. Thus, the equilibrium brush structure is characterized by the coexistence of relatively small spherical domains of collapsed polymer immersed in a matrix of nearly pure solvent.

The results of this paper indicate that normal deformation of the brush leads to the rearrangement of equilibrium micelle structure: stretching leads to an increase in both the numbers of chains f and the micelle size D, whereas compression results in the decrease in f and D (see Table 2). Figure 5 demonstrates schematically the dependence of the number of chains f in a micelle on deformation (all the chains are the bridging chains). As seen in Figure 5, f increases with increasing H for both compressed and stretched brushes and passes through the maximum at high stretching comparable to that in a totally stretched string of thermal blobs, $H \cong N\tau$. This rearrangement of micelle structure with deformation has purely equilibrium character: a minimum of the system free energy is attained when the aggregates increase their size with H increasing.

The results of this paper indicate also that the relative fluctuations of the number of chains per micelle is small (see Appendix). The globular cores of stretched pinned micelles are localized in the middle of the gap between two surfaces, and their positions fluctuate only slightly. This is the consequence of the structure of the pinned

micelles. Due to the small size of the core as compared to the overall micelle size, $R \ll D$, the legs are tilted with respect to the normal direction on the surface. The maximum value of their lateral projections is $D \cong \sqrt{sf}$. This provides the minimum of the effective potential in the middle of the gap.

2. Scenarios of Brush Deformation. We have shown that the equilibrium reorganization of collapsed brush structure in the process of deformation depends of the relationship between the normalized grafting area per chain s/N and the well-known parameter of volume interaction $\tau N^{1/2}$.

For the compression of a brush one can predict four different scenarios of molecular reorganization with a decrease in H.

(c1) $s/N < (\tau N^{1/2})^{-1}$: The brush is initially homogeneous and remains as such under compression.

(c2) $(\tau N^{1/2})^{-1} < s/N < 1$: The spherical cores of the pinned micelles are compressed into pancakes. The pancakes merge into the homogeneous brush when H reduces to the height of a homogeneous brush with the same values of s, N, and τ.

(c3) $1 < s/N < (\tau N^{1/2})^{2/3}$: Pinned micelles are compressed into pancakes, decreasing in dimensions (transition to one-chain-globule regime).

(c4) $s/N > (\tau N^{1/2})^{2/3}$: The individual globules are compressed.

For stretching of the brush we have three qualitatively different scenarios. The reorganization with an increase in H is as follows.

(s1) $s/N \leq (\tau N^{1/2})^{-2}$: The polymer-rich phase in the layer remains continuous and fluctuates along the height of the gap, its volume fraction decreasing until the brush decomposes into individual stretched chains.

(s2) The brush forms stretched pinned micelles positioned in the middle of the gap; the micelles transform with stretching before decomposing into individual stretched chains. This may happen starting from an initially homogeneous layer (if $(\tau N^{1/2})^{-2} < s/N < (\tau N^{1/2})^{-1}$), or from an undeformed pinned micelle structure (if $(\tau N^{1/2})^{-1} < s/N < (\tau N^{1/2})^{1/3}$), or from a system of individual globules (if $(\tau N^{1/2})^{2/3} < s/N < (\tau N^{1/2})^{4/3}$).

(s3) $s/N > (\tau N^{1/2})^{4/3}$: The individual globules increase their extension and transform into individual stretched chains without producing micelles.

It is worth noting that an increase in H pushes the brush into the SPM regime both from the regime of the homogeneous brush at high grafting density and from the mushroom regime at low grafting density. In the last case this effect is due to the fact that elongation of legs with increasing H causes an increase in lateral elasticity of legs.

Stretching of the brush in the pinned micelle regimes leads to the monotonous dependence of restoring force on the elongation H. The restoring force (per unit surface area) $\mathbf{f} = (1/s)(dF_m/dH)$ in the pinned micelles regime is equal to

$$\mathbf{f} = \frac{\tau kT}{s}\left(1 - \frac{D^{5/4}}{H^{5/4}}\right) \quad \text{SPM1 regime} \qquad (41a)$$

$$\mathbf{f} = \frac{\tau kT}{s}\left(1 - \frac{H_0^{1/2}}{H^{1/2}}\right) \quad \text{SPM2 regime} \qquad (41b)$$

$$\mathbf{f} = \frac{\tau kT}{s}\cdot\frac{H}{D} \quad \text{PM regime} \qquad (41c)$$

These equations are obtained using the scaling formulas for F_m shown in Table 2. The values of f, R, and D in (41) refer to the undeformed pinned micelle, the value H_0 in (41b) is the thickness of an undeformed homogeneous brush. For the $\mathbf{f} = \mathbf{f}(H)$ dependences for globular and homogeneous brush states see refs 16, 17, and 20.

3. Interactions of Brushes and Hysteresis Effects. For the process of deformation to be quasi-equilibrium, the micellar structures have to rearrange. This process involves overcoming considerable activation barriers, the magnitude of which depends on the parameters of the brush (N, τ, s). For long chains this can result in actual "freezing" of the initial system and deformation of such brushes will occur without rearranagement of the pinned micelles formed in the undeformed layer. The peculiar structure of the brush in the regime of pinned micelles and its extremely slow kinetics can manifest themselves experimentally in the force measurements in the form of hysteresis effects in the force versus deformation curves. We expect this to be especially pronounced in the case of interaction between two identical brushes oriented face to face.

Let us consider first the equilibrium conditions. It is easy to see that the more favorable state corresponds to the formation of joint micelles comprising the grafted chains from both surfaces, provided $H/2 < sf$. The system in this case is equivalent to the stretched brush with bridging chains in regime PM.

The free energy per chain in a joint micelle is (cf. (29))

$$\frac{F_m}{kT} = \tau\sqrt{sf + \frac{H^2}{4}} + \frac{1}{2}(2N)^{2/3}\tau^{4/3}f^{-1/3} \qquad (42)$$

where $f_j = f/2$, is the number of chains in a joint micelle (f is the effective number). Taking into account the numerical coefficients, we obtain after minimization of F_m (at $H^2 < 4sf$)

$$(F_m)_j \cong 2^{-2/3}F_0\left(1 + k\frac{H^2}{sf}\right) \qquad (43)$$

where F_0 is the free energy per chain in a micelle in an individual brush and $k > 0$ is the numerical coefficient of order 1.

Hence in equilibrium, at small enough separations H, the joint micelles are favorable, $F_j < F_0$. The micelle legs act as elastic strings (F_j decreases with decrease in H) and hence two brushes attract each other. This equilibrium attraction takes place at distances H of the order of lateral size of a micelle $D \approx \sqrt{sf}$. Note that $D \gg R_0$, where R_0 is the radius of the micelle core ($2R_0$ is, therefore, the thickness of the original brushes).

However, due to high potential barriers preventing the rearrangements and formation of equilibrium micelles, the joint micelle will be most probably formed by merging two pre-existent micelles upon their immediate contact. The merging of individual micelles occurs, thus, at $H \cong 4R_0$ and leads to the formation of one core of radius $\tilde{R}_0 = 2^{1/3}R_0$ (instead of two cores of radius R_0), attached to the surfaces by $2f_0$ legs with the normal projection of size $(H - 2\tilde{R}_0)/2$. The free energy per unit area is then given by

$$\tilde{F}/kT \cong s^{-1}\left[\tau\sqrt{f_0 s + (H/2 - \tilde{R}_0)^2} + \frac{N^{2/3}\tau^{4/3}}{(2f_0)^{1/3}}\right] \qquad (44)$$

and, correspondingly, the attractive force (per unit area) between the two surfaces scales as

$$G = \frac{1}{kT}\frac{\partial \tilde{F}}{\partial H} \cong \frac{\tau(H/2 - \tilde{R}_0)}{(f_0 s + (H/2 - \tilde{R}_0)^2)^{1/2}} \quad (45)$$

This attractive force appears at $H/2 \cong 2R_0$ and then decreases to zero at $H/2 = \tilde{R}_0$. Further compression of the brushes leads to the appearance of a repulsive force opposing brush compression.

If one starts separating the two brushes after the joint micelles are formed, the attractive force will exist at $H > 2\tilde{R}_0$ and will be still given by (45). However, this force continues to act at the distances $H > 4R_0$ as well, since the free energy per unit area with the joint micelle formed (eq 44) is still smaller than the free energy of the two separated brushes (eqs 9–12). Only at $H/2 \cong \sqrt{f_0 s} \cong D_0$ do both free energies become equal, does the joint micelle disintegrate, and do the brushes not interact any more. Thus, the attractive force has the maximum range $H/2 \cong D_0$, much larger than the thickness of a brush R_0, but it will manifest itself only upon separation of two surfaces which were previously brought close enough together.

The expected hysteresis in the dependence of the force on deformation is shown schematically in Figure 6. (Arrows show the force behavior during each compression-stretching cycle if the final value of H is sufficiently high, $H \gg D$). Since $D_0 \gg R_0$ for the pinned micelles, these hysteresis effects can be probably investigated experimentally. As seen from Table 2, the range of the hysteresis (the difference between D_0 and R_0) increases with the area per chain, s, and with the inferior solvent strength.

One might expect some interesting experimental observations upon shearing of such brushes, as the shear force will monitor the lateral inhomogeneity of the brush structure.

Acknowledgment. E.B.Z., T.M.B., and V.A.P. acknowledge the International Science Foundation, the Russian Government (Grants NT 8000, NT 8300), and the Russian Foundation for Fundamental Investigations (Grant 93-03-5797) for financial support.

Appendix: Fluctuations in the Micelle Structure

Let us show now that the pinned micelles have a well-defined structure with only small fluctuations of both the position and the dimension of the micelles. The scaling approximation allows one to estimate the fluctuations around the average values. We consider the fluctuation of the core center position in a pinned micelle in the SPM and PM regimes. The free energy of a micelle with its center located at the height h from one of the surfaces can be estimated as

$$\frac{F_m f}{kT} \cong f\tau[\sqrt{h^2 + fs} + \sqrt{(H-h)^2 + fs}] + \tau^{4/3}N^{2/3}f^{2/3}\left[1 - \left(\frac{f}{N^{1/2}\tau}\right)^{2/3}\right] \quad (A1)$$

The minimal value of $F_m f$ corresponds to $h = h_0 = H/2$. Assuming a narrow Gaussian distribution of h around h_0, one can estimate the square averaged deviation from h_0, $\langle \delta h^2 \rangle = \langle (h - h_0)^2 \rangle$ as

$$\langle \delta h^2 \rangle \cong (kT)^{-1}\left(\frac{\partial^2 (F_m f)}{\partial^2 h}\right)_{h_0}^{-1} \cong \frac{(H^2 + fs)^{3/2}}{\tau s f^2} \quad (A2)$$

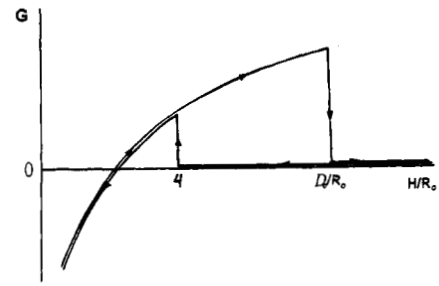

Figure 6. Schematic representation of the hysteresis effect during the interaction between two laterally inhomogeneous brushes. $G > 0$ = attractive forces. Arrows indicate the dependence of force via deformation during each compression–stretching cycle.

Using the scaling formulas for f from Table 2, one has for the regimes SPM and PM

$$\delta h/H \cong s^{1/4}\tau^{-3/4}H^{-1/4}N^{-1/2} \quad \text{regime SPM1} \quad (A3a)$$

$$\delta h/H \cong sH^{-1}N^{-1/2} \quad \text{regime SPM2} \quad (A3b)$$

$$\delta h/H \cong s^{2/5}\tau^{-3/5}H^{-1}N^{-1/5} \quad \text{regime PM} \quad (A3c)$$

where $\delta h = \sqrt{\langle \delta h^2 \rangle}$. One can see from (A3) that the relative fluctuation of the core position decreases with increasing H and decreasing s. The estimations show that these values are small in the major part of the PM and SPM regions, provided $\tau N^{1/2} \gg 1$. Note that in the neighboring SG regime fluctuations of the core position are expected to be much larger, $\delta h/H \cong 1$.

Fluctuations $\langle \delta f^2 \rangle = \langle (f - f_0)^2 \rangle$ of the number of chains in a pinned micelle around the average and more probable value f_0 were calculated in ref 7 to be $\langle \delta f^2 \rangle \approx (\partial^2 (F_m f)/\partial f^2)^{-1}$. It follows that $\langle \delta f/f_0 \rangle \cong ((F_m(f)/kT)f_0)^{-1/2}$ where $F_m(f)$ is the f-dependent part of free energy of a chain in a micelle. Using the appropriate values of $F_m(f)$ and f_0 from Table 2 one obtains

$$\delta f/f_0 \cong s^{1/4}\tau^{-3/4}N^{-1/2}H^{-1/4} \quad \text{regime SPM1} \quad (A4a)$$

$$\delta f/f_0 \cong s^{-1}N^{-1/2}H^{-1} \quad \text{regime SPM2} \quad (A4b)$$

$$\delta f/f_0 \cong s^{1/5}\tau^{-4/5}N^{-3/5} \quad \text{regime PM} \quad (A4c)$$

$$\delta f/f_0 \cong s^{1/8}\tau^{-7/8}N^{-3/8}H^{-3/8} \quad \text{regime CPM} \quad (A4d)$$

where $\delta f = \sqrt{\langle \delta f^2 \rangle}$.

Equations A4 show that the fluctuations in the number of chains per micelle are small in all four regimes provided that $f_0 \gg 1$; i.e. the pinned micelles are indeed well-defined structures.

References and Notes

(1) Borisov, O. V.; Zhulina, E. B.; Birshtein, T. M. *Polym. Sci. USSR* **1988**, *30*, 767.
(2) Halperin, A. *J. Phys.* **1988**, *49*, 547.
(3) Zhulina, E. B.; Priamitsyn, V. A.; Borisov, O. V. *Polym. Sci. USSR* **1989**, *31*, 205.
(4) Zhulina, E. B.; Borisov, O. V.; Priamitsyn, V. A. *J. Colloid Interface Sci.* **1990**, *137*, 295.
(5) Zhulina, E. B.; Borisov, O. V.; Priamitsyn, V. A.; Birshtein, T. M. *Macromolecules* **1991**, *24*, 140.
(6) Shim, D. F. K.; Cates, M. E. *J. Phys.* **1989**, *50*, 3535.
(7) Klushin, L. I. Preprint, 1992.
(8) Williams, D. R. M. *J. Phys. II* **1993**, *3*, 1313.
(9) Ross, R. S.; Pincus, P. *Europhys. Lett.* **1992**, *19*, 79.
(10) Yeung, C.; Balazs, A. C.; Jasnow, D. *Macromolecules* **1993**, *26*, 1914.

(11) Tang, H.; Szleifer, I. Preprint, 1994.
(12) Soga, K. G.; Guo, H.; Zuckermann, M. J. *Europhys. Lett.* **1995**, *29*, 531.
(13) Grest, G. S.; Murat, M. *Macromolecules* **1993**, *26*, 3108.
(14) Lai, P. Y.; Binder, K. *J. Chem. Phys.* **1992**, *97*, 586.
(15) Zhao, W.; Krausch, G.; Rafailovich, M. H.; Sokolov, J. *Macromolecules* **1994**, *27*, 2933.
(16) Halperin, A.; Zhulina, E. B. *Macromolecules* **1991**, *24*, 5393.
(17) Zhulina, E. B.; Halperin, A. *Macromolecules* **1992**, *25*, 5730.
(18) Williams, C.; Brochard, F.; Frish, H. L. *Annu. Rev. Phys. Chem.* **1981**, *32*, 433.
(19) de Gennes, P. G. *Scaling Concepts in Polymer Physics*; Cornell University Press: Ithaca, NY, 1885.
(20) Halperin, A.; Zhulina, E. B. *Europhys. Lett.* **1991**, *15*, 417.

MA950395K